CORE
Metadata, citation and similar papers at core.ac.uk
Provided by Universidade do Minho: RepositoriUM

Vacuum 82 (2008) 1507–1511

Contents lists available at ScienceDirect

Vacuum

journal homepage: www.elsevier.com/locate/vacuum

Influence of oxygen/argon pressure ratio on the morphology, optical and electrical properties of ITO thin films deposited at room temperature

Hai-Ning Cui [a,1], V. Teixeira [a,*], Li-Jian Meng [b], R. Martins [c], E. Fortunato [c]

[a] Departamento de Física/CFUM, Universidade do Minho, 4800-058 Guimarães, Portugal
[b] Departamento de Física, Instituto Superior de Engenharia do Porto, Rua de São Tomé, 4200 Porto, Portugal
[c] Departamento de Ciência dos Materiais/CENIMAT, Universidade Nova de Lisboa, Quinta da Torre, 2829-516 Caparica, Portugal

Keywords:
Indium tin oxide
DC sputtering
Optical and electrical properties
Free carrier density (n_c)
The carrier mobility (μ) of the ITO film

A B S T R A C T

Transparent conductive oxides (TCOs) such as indium tin oxide (ITO) thin films onto glass substrates are widely used as transparent and conductive electrodes for a variety of technological applications including flat panel displays, solar cells, smart windows, touch screens, etc.
ITO films on glass and polycarbonate (PC) substrates were prepared at room temperature (RT) and at different P_{O_2}. The films were characterized in terms of the surface roughness (δ), sheet resistance, the refractive index (n) and extinction coefficient (k). The free carrier density (n_c) and the carrier mobility (μ) of the ITO (In_2O_3:Sn) films were measured and studied. The n_c and μ values vary in different ratio of oxygen partial pressure (P_{O_2}) of ITO deposition. The observed changes in the ITO film resistivity are due to the combined effect of different parameter values for n_c and μ. From AFM analysis and spectra calculations, the surface roughness values of the ITO films were studied and it was observed that the δ values were lower than 15 nm. The energy band gap E_g ranges from 3.26 eV to 3.66 eV as determined from the absorption spectrum. It was observed an increase on the energy band gap as the P_{O_2} decrease in the range of 20–2% P_{O_2}. The Lorentz oscillator classical model has also been used to fit the ellipsometric spectra in order to obtain both refractive index n and extinction coefficient κ values.
© 2008 Elsevier Ltd. All rights reserved.

1. Introduction

Transparent conductive oxides (TCOs) are of great importance for silicon based and most other thin film solar cells. Indium tin oxide (ITO) thin films onto glass substrates are widely used as transparent and conductive electrodes for a variety of technological applications including flat panel displays, solar cells, smart windows, touch screens, etc.

Generally a high optical transmission from visible to near infrared (NIR) wavelength and a low sheet resistance (R_s) characterize a high-quality film of indium tin oxide (ITO) [1–3].

ITO is a wide-gap, degenerated semiconductor where electrons are the major charge carriers. The Sn atoms are considered to substitute for In, without ordering. The difference of valence between In^{3+} and Sn^{4+} results in the donation of a free electron to the lattice. For most applications, the ITO films must be as conducting as possible, which requires a high carrier density (n_c) and a high carrier mobility (μ). As a part of a research to develop new flexible multilayered electrochromic devices prepared by dc magnetron sputtering, we are investigating ITO used as the transparent electrodes. The attainment of these properties is strongly dependent on the growth condition-oxygen partial pressure ratio (P_{O_2}). Among the technologies available for ITO thin film production, magnetron sputtering is the most widely investigated and large-scale deposition equipment is available [2–4]. Moreover, the replacement to flexible polymer substrates is gaining a great interest because it can give advantages such as lighter weight, higher shock resistance and scalable roll-to-roll deposition processes. In this work ITO thin films were prepared by dc magnetron sputtering technique, mainly because a high sputtering rate associated with good film properties and low substrate temperatures can be achieved. In our previous study [3], the optimum r.f. diode sputtering was used for the deposition of ITO. Physical properties such as the free carrier density (n_c), the carrier mobility (μ) and various optical parameters of the ITO films are important criteria to describe the characteristics, microstructure and physical properties of the films. These parameters are also sensitive to the microstructure and have a strong influence on the application of the coating. Therefore, it is important to study the influence of P_{O_2} on the micro and electronic parameters (μ and n_c), energy band gap E_g, sheet resistance, surface roughness (δ), refractive index and extinction coefficient of the ITO film.

* Corresponding author.
E-mail address: vasco@fisica.uminho.pt (V. Teixeira).
[1] Present address: College of Physics, JiLin University, 2519 JieFangDaLu Road, ChangChun 130021, PR China.

0042-207X/$ – see front matter © 2008 Elsevier Ltd. All rights reserved.
doi:10.1016/j.vacuum.2008.03.061

2. Experimental details

A home made system of DC magnetron reactive sputtering was used to deposit the ITO films. Further details about the experimental set up have been reported elsewhere [5]. The sputtering target is composed of 10 wt% SnO_2-doped In_2O_3. The base pressure of the vacuum chamber was less than 1×10^{-3} Pa by mechanical and oil diffusion pumps before deposition. The oxygen partial pressure ratio is defined as $P_{O_2} = P(O_2)/[P(O_2) + P(Ar)]$, where $P(O_2)$ and $P(Ar)$ are the gas pressures. P_{O_2} is adjusted from 0% to 27%. The sputtering power applied was 90 W. All films were deposited at room temperature.

The film transmittance, absorbance, diffuse and specular reflectance were measured in UV–visible–near infrared (UV–vis–NIR) region by a double beam spectrophotometer of Shimadzu UV-3101PC, which is available for various measurements over a wavelength range of 200–3200 nm. The film resistivity was measured by Veeco FPP-5000 four-point probe. The carrier concentration (n_c) and Hall mobility (μ) were determined from Hall effect measurements using the Van der Pauw geometry (a four-point probe square configuration, 5 mm side with Cr contacts deposited by thermal evaporation assisted by electron gun) on a BIORAD HL5500 system with a permanent magnet of 5 kG. The microstructures of the film surface were determined by atomic force microscopy (AFM, Multimode TM SPM 3, Digital Instruments Nanoscope).

3. Results and discussion

An overview of the results of the ITO films is shown in Table 1. In the following sections we present and discuss the results obtained for the ITO sputtered films.

3.1. Transmission spectra of ITO films

The transmission spectra of some as-deposited ITO films are shown in Fig. 1. The transmission curves in the long wavelength (NIR: near infrared) region shift to red direction and increases with increasing P_{O_2} except for the lowest P_{O_2} sample (2%). This behaviour indicates an increase of the amount of free electrons with decreasing P_{O_2}, because the electrons are from oxygen vacancies in ITO film [6]. In general it is observed that the near infrared transmittance decrease as the film thickness increases. These changes of the optical properties are consistent with the changes observed in the electrical properties, mainly the ones associated with the increase of the carrier concentration (see Table 2), which lead to a lower value associated with the plasma frequency. Further discussion is presented in Section 3.3.

The optical properties of the ITO films are determined to a large extent by the microstructure of the film and hence by the preparation technique. It is stated that the decrease of the transmittance at lower P_{O_2}, which is smaller than the optimum 10% P_{O_2}, is due to the formation of non-stoichiometric films. As P_{O_2} is increased, the film structure may also vary from a dense structure into a columnar or cluster structure with more pronounced voids [7]. All these could result in an increase of the film transmittance. All the values of the transmission of the as-deposited ITO films are above 83% in the range of 470–1900 nm. From Table 1, it can be observed that the optimum depositing conditions of 10% and 12% P_{O_2} result in a high transmission of 95% with the lowest R_s. Although this value of transmittance is not as high as that of sample a1 (27% P_{O_2}), it should be good enough for opto-electronic applications such as electrochromic switching devices.

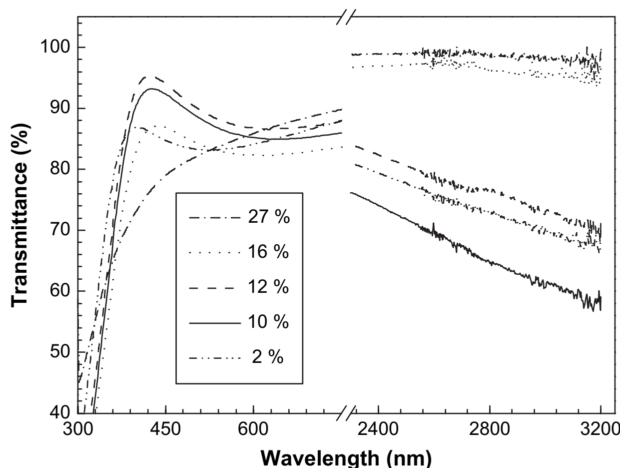

Fig. 1. Transmittance spectra of films prepared with different oxygen partial pressure ratio.

The fundamental physical properties and mechanisms governing the optical performance of the transparent conducting ITO films could be described by interband absorption, logarithmic band edges, electron scattering and phonon absorption. In the ultraviolet region, the absorption is strong due to excitations across the fundamental band gap E_g. Substitutional doping of Sn on In sites in the In_2O_3 lattice shifts E_g towards shorter wavelengths. This phenomenon is due to the Burstein–Moss effect, i.e. a blocking of the lowest states in the conduction band, which is partly balanced by many-body effects. The optical properties around E_g are complicated by the occurrence of logarithmic band edges, often referred to as 'Urbach tails', which give some weak absorption at the blue end of the luminous spectrum. Urbach tails are common features in semiconductor materials, and their origin has been the subject of much speculation. It appears that several physical mechanisms can contribute, and that one of them is associated with the existence of Sn^+ acting as an ionized impurity. The free electrons in the In_2O_3 lattice undergo scattering, whose strength limits ρ as well as the infrared reflectivity of ITO. In principle, there are many types of scattering centres that have to be considered, including ionized and neutral impurities, phonons and dislocations.

3.2. Sheet resistance and Figure of Merit

The lowest value of the sheet resistance (R_s) of the ITO films was obtained when the deposition time (t_d) was 2 min. The obtained

Table 1
Deposition conditions and parameters for ITO films

Sample	P_{O_2} (%)	t_d (min)	d_e (nm)	T_{max} (%)	R_s (Ω/Sq.)	δ (nm)	E_g (eV)	Φ_{max} ($\times 10^{-3}\ \Omega^{-1}$)
a1	27	0.7	–	99.6	∞	13.6	–	–
a2	25	0.7	–	99.5	∞	13.2	3.53	–
a3	21	0.7	–	99.3	760.2	11.2	3.49	1.3
a4	16	2	48	97.0	654.0	12.2	3.48	1.5
a5	12	2	94	95.0	108.7	11.5	3.53	8.7
a6	10	2	91	95.0	99.9	12.2	3.62	9.4
a7	2	2	66	94.0	132.8	13.6	3.66	7.1
a8	0	2	–	93.0	137.6	11.9	3.26	6.8

Note. P_{O_2}: ratio of oxygen partial pressure; t_d: deposition time; d_e: thickness obtained by fitting ellipsometric parameters; T_{max}: transmittance at maximum; R_s: sheet resistance; δ: surface roughness; E_g: energy band gap; Φ_{TC}: Figure of Merit.

Table 2
The ρ, n_c and μ of the ITO films for different P_{O_2}

Sample	ρ (Ω cm)	n_c (cm^{-3})	μ (cm^2/V s)	P_{O_2} (%)	d_e (nm)
i1	9.12×10^{-2}	5.23×10^{18}	13.1	16	47.9
i2	6.01×10^{-4}	7.89×10^{20}	13.2	12	93.9
i3	5.93×10^{-4}	7.44×10^{20}	14.1	10	90.5
i4	9.39×10^{-4}	4.54×10^{20}	14.6	2	66.2

value was 99.9 Ω/Sq. (Ohm/Square) for 10% P_{O_2}. An increase in R_s on either side of the optimum 10% P_{O_2} was observed after increasing and decreasing P_{O_2}. From the above, the R_s of the as-deposited ITO film is sufficiently low to be used as an electrode layer for electrochromic devices.

At lower than the optimum P_{O_2} the film resulted in higher R_s, which is due to the formation of non-stoichiometric films. At higher than the optimum P_{O_2} the larger R_s could be due to additional oxygen accumulated at the grain boundaries that act as scattering centres to electrons. Table 1 shows the Figure of Merit ($\Phi_{TC} = T_{max}/R_s$) [8] of the films too and the best one with the lowest R_s, is sample a6, $\Phi_{TC} = 9.4 \times 10^{-3}\ \Omega^{-1}$. No post-annealing was done in the process of the film synthesis. Considering industrial applications, this will be less expensive and more practical to produce some device applications, especially when sensitive layers are present or polymer substrates are used.

3.3. Carrier concentration and carrier mobility

The carrier concentration (n_c), carrier (or Hall) mobility (μ) and resistivity (ρ) of the ITO films were measured. Table 2 shows some parameters such as ρ, n_c and μ for the ITO sputtered films produced at different P_{O_2} s. The increase in the resistivity is due to the decrease in both n_c and μ with increasing P_{O_2} for the range of 2–16%. Obviously an increase of ρ on either side of the optimum 10% P_{O_2} was observed. Similar to the explanation given in Section 3.1, at lower values than the optimum 10% P_{O_2} the higher ρ could result from the phases of metal oxide other than In_2O_3 doped SnO_2. The resulting film is non-stoichiometric. Another possible justification is that because the amount of pores (or defects) in the sample i4 is small, it decreases the scattering of the charge carriers, and then its mobility increases to 14.6 $cm^2/V\,s$. From the decrease of the carrier mobility of the films among all samples i1–i4, we can conclude that the amount of pores increases with the increasing of P_{O_2} during the deposition of the ITO films. At higher values than the optimum 10% P_{O_2} the larger ρ could be due to (i) additional oxygen accumulating at the grain boundaries and then acting as scattering centres for electrons and (ii) swelling structure of the film changing the carrier concentration (n_c). The smaller value 13.1 $cm^2/V\,s$ mobility of sample i1 is due to the larger amount of pores or defects, and it depends on the growing conditions and characteristics of the thin film. With increasing thickness (in the range up to 100 nm) it was observed that the film resistivity decreases. For the ITO sputtered films an increase in the carrier concentration was observed suggesting that for thinner films the resistivity is controlled by a large amount of grain boundaries associated with the film growth (which show typically a columnar type) which limits the effective carrier concentration.

These experimental data show that the value for carrier mobility and carrier concentration is very sensitive to the structure of the films. The carrier concentration increases when the oxygen content decreases from 16% to 12% P_{O_2}. The increase of P_{O_2} enhances the pore formation in the film and then the mobility of the carrier becomes lower at high P_{O_2}, from 2% to 16%, especially for sample i1. The carrier (Hall) mobility seems to increase with film thickness within the range studied.

3.4. Surface roughness

The surface morphology of the ITO films is not easy to achieve by using SEM technique, because the film is too smooth and very thin to be observed using conventional SEM equipment. In this work a calculation method was used to study the surface morphology from the UV–vis–NIR spectra.

The δ parameter corresponds to the standard deviation of the micro-geometric surface height (or peaks and valleys). It can be obtained from the total integrated scattering (TIS). The TIS is defined as the ratio of the light scattered by diffuse reflectance to the total reflectance (specular plus diffuse reflectance) of the surface [9,10]. If the surface roughness δ is much smaller than the wavelength λ, and θ_0 is the angle of incidence, then

$$\delta = \frac{\lambda}{4\pi \cos\theta_0}(\mathrm{TIS})^{1/2}. \quad (1)$$

We can calculate the δ value by Eq. (1). Fig. 2 shows the diffuse reflectance, specular reflectance and TIS spectra of the ITO films over a wavelength range of 300–810 nm. The δ values of the samples are summarized in Table 1. Fig. 3 is a typical AFM micrograph of the surface microstructure and nanotopography of the ITO film. As can be seen in Table 1 the surface roughness ranges from 11.2 nm to 13.6 nm. A small increase in the surface roughness was obtained for higher P_{O_2} (27%) and lower P_{O_2} (2%). In the classical theory the loss of light passing through optical films can be caused by two factors, absorption and scattering. The light scattering can be caused by the surface micro-roughness and by scattering at the film grain boundaries. The surface roughness and the nanoscale grain boundaries are clearly seen by AFM in Fig. 3. The measured grain size is 30 nm and the average height of δ is less than 15 nm, which is in very good agreement with the roughness obtained from Eq. (1).

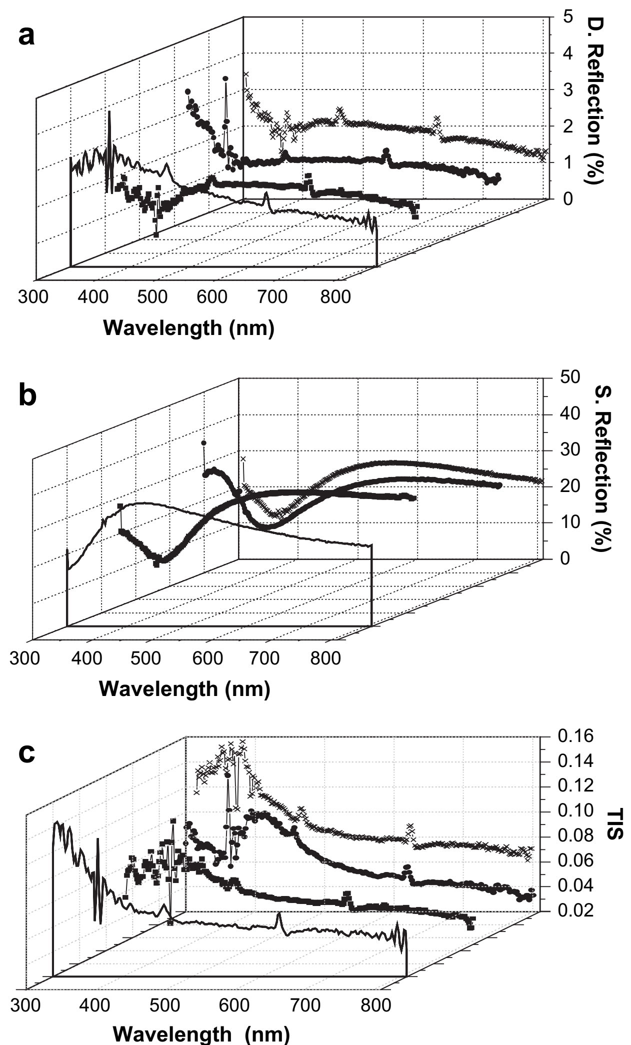

Fig. 2. (a) Diffuse reflectance; (b) specular reflectance and (c) TIS spectra of ITO films over a wavelength range of 300–810 nm in different oxygen partial pressure (P_{O_2}); solid line: 27% P_{O_2}, square: 16% P_{O_2}, circle: 10% P_{O_2}, cross: 2% P_{O_2}.

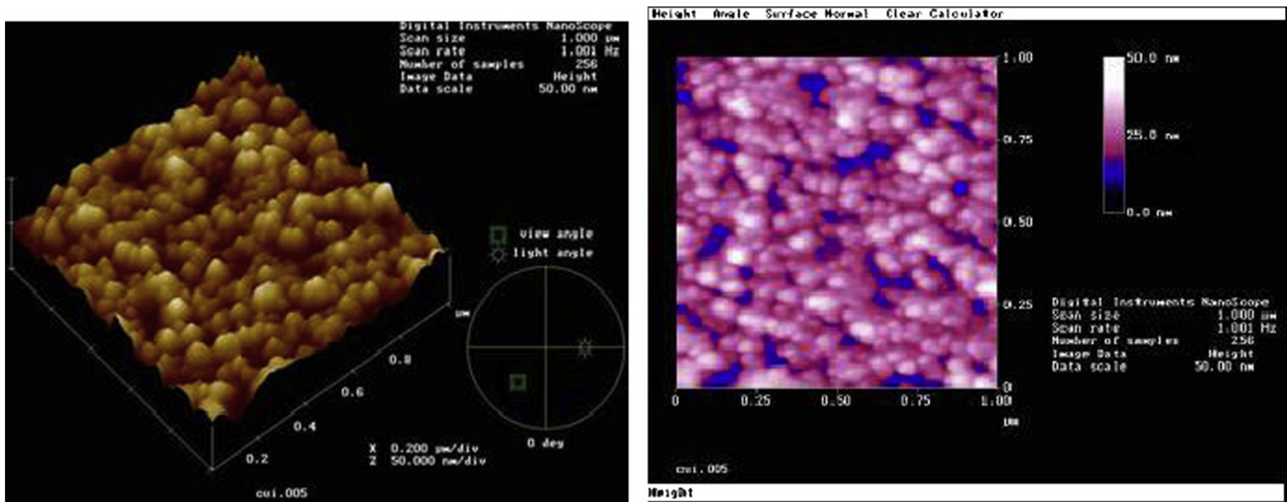

Fig. 3. AFM micrograph showing the typical surface morphology for an ITO film (sample a6) deposited with 10% ratio of oxygen partial pressure.

Since the as-deposited ITO sample is a good transparent thin film (transmission above 83% in the range of 470–1900 nm), we suppose that the scattering mainly comes from the interfaces of the film.

3.5. Refractive index and extinction coefficient

It has been found that the film transmittance increases with increasing P_{O_2}. This behaviour is caused mainly by two reasons, one is the variation of the refractive index (n), another is the variation of the extinction coefficient (κ). Meng et al. studied the dispersion of n of the tin oxide films prepared at different total pressures and P_{O_2}, using the transmission spectra [11]. Several methods have been used to determine the optical constants of thin films based on the measurement of intensity of the reflected, absorbed and/or transmitted light as a function of wavelength and/or angle of incidence [12,13].

Among these methods, the one given by Swanepoel is widely used because of its simplicity [14,15]. The Lorentz oscillator classical model has also been used for fitting the ellipsometric spectra in order to obtain the n and κ values.

The dispersions of n and κ of the films prepared with 2.1×10^{-1} Pa P_T and different P_{O_2} are shown in Fig. 4. The n and κ values of the films over a wavelength range of 400–800 nm were plotted against the photo-energy (3.2–1.4 eV). It can be seen that the sample prepared at high P_{O_2} shows a different behaviour compared to the samples prepared at low P_{O_2}. This can be related with the variation of the structure of the films. The κ of sample i3 at wavelength 700 nm is 0.034 using ellipsometric measurements (Fig. 4b).

3.6. Energy band gap

There are different models and many reports about the absorption coefficient and energy band gap (E_g) [6]. In this study we have calculated E_g values using the direct transition model ($N=2$) by $\alpha^N = C(h\nu - E_g)$. Table 1 shows the E_g values of the ITO films.

The intrinsic E_g of the ITO material is 3.53 eV [16]. The obtained values of the films vary between 3.26 and 3.66 eV and increases as the oxygen pressure decreases in the range of 20–2% P_{O_2}. Samples a6 and a7 in Table 1 show comparably high effective E_g, possibly this is caused by a combination of Burstein–Moss-Shift [17] and contributions of scattering [18]. It should be as following, $E_g = E_{g,0} + \Delta E_{BM} = E_{g,0} + \hbar(3\pi^2 n_e)^{2/3}/2m^*_{vc} + \hbar\Sigma$, where E_g is the measured or varied effective band gap, $E_{g,0}$ is the intrinsic band gap, m^*_{vc} represents the reduced effective mass and n_e is free electron density. The $\hbar\Sigma$ represents the broadening of the band gap due to scattering and widening of the transition. It is assumed that the Sn^{4+} ions behave as single charged point scatter too, except the boundary scatter. We can observe that the ΔE_{BM} value comes from

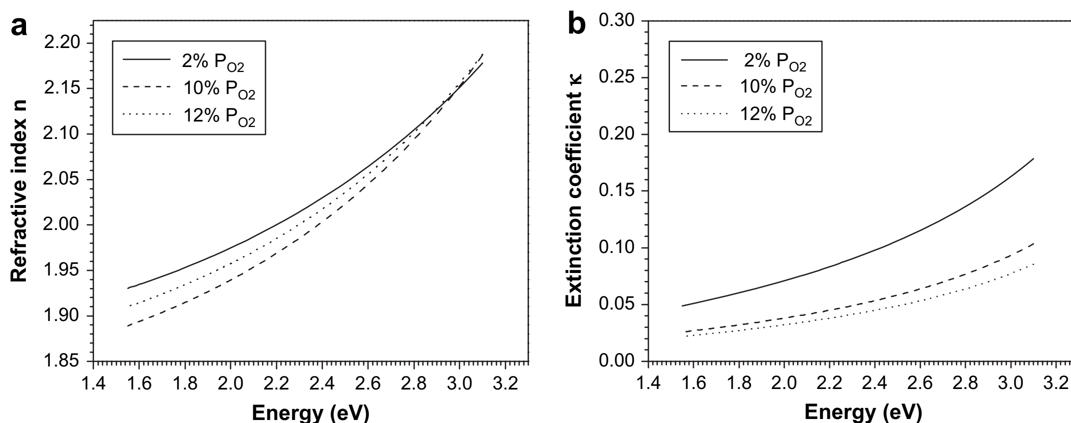

Fig. 4. Refractive index n (a) and extinction coefficient κ (b) for wavelengths in the range 400–800 nm for ITO films prepared with different oxygen partial pressures.

the contribution of both $\hbar\Sigma$ and $\hbar(3\pi^2 n_e)^{2/3}/2m^*_{vc}$. For other samples that have comparably low effective E_g (<3.53 eV), this is possibly caused by the structure of non-stoichiometric when the ITO films were deposited at higher or lower P_{O_2}. From the above discussion the variant E_g value of the ITO film cannot be explained by using only a Burstein–Moss-Shift which was also analysed by Bender et al. mentioned [6].

4. Conclusions

Transparent ITO thin films on glass substrates prepared at different P_{O_2}s show different values for the surface roughness (δ), sheet resistance, the refractive index (n) and the extinction coefficient (κ). All values of the transmission for the as-deposited ITO films are above 83% in the range of 470–1900 nm. The film maximum transmittance increases from 93% to 99% when increasing P_{O_2}. The film surface roughness was in the range of 11.2–13.6 nm. The lowest value for sheet resistance (R_s) of the ITO films deposited at RT was 99.9 Ω/Sq. for 10% P_{O_2}. The free carrier density (n_c) and the carrier mobility (μ) of the ITO (In_2O_3:Sn) films were measured. The n_c and μ values vary with different ratios of oxygen partial pressure (P_{O_2}) of ITO deposition. The carrier concentration increases from 5.23×10^{18} cm^3 to 7.89×10^{20} cm^3 when the oxygen pressure decreases from 16% to 12% P_{O_2}. The carrier mobility increases from 13.1 cm^2/V s to 14.6 cm^2/V s when the oxygen pressure decreases from 16% to 2% P_{O_2}. The ITO energy band gap E_g ranges from 3.26 eV to 3.66 eV. An increase in the band gap was observed as the oxygen pressure decreases in the range of 20–2% P_{O_2}.

Acknowledgments

H.N. Cui acknowledges the F.C.T.-Fundação para a Ciência e Tecnologia grant from Portugal.

References

[1] Lewis Brian G, Paine David C. Applications and processing of transparent conducting oxides. MRS Bull August 2000:22–7.
[2] Limmer SJ, Cruz SV, Cao GZ. Appl Phys A 2004;79:421–4.
[3] Cui H-N, Xi S-Q. Thin Solid Films 1996;288:325–9.
[4] Takaki S, Matsumoto K, Suzuki K. Appl Surf Sci 1988;33/34:919–25.
[5] Almeida JB. Vacuum 1989;39:717–21.
[6] Bender M, Seelig W, Daube C, Frankenberaer H, Ocker B, Stollenwerk J. Thin Solid Films 1998;326:72–7.
[7] Cui Hai Ning, Teixeira V, Monteiro A. Vacuum 2002;67:589–94.
[8] Ohring Milton. The materials science of thin films. San Diego: Academic Press Inc; 1992. p. 454.
[9] Guenther KH, Wieder PG, Bennett JM. Appl Opt 1984;23:3820.
[10] Bennett HE, Porteus JO. J Opt Soc Am 1961;51:123.
[11] Meng LJ, Santos MP. Vacuum 1994;45(12):1191–6.
[12] Klein JD, Yen A, Cogan SF. J Appl Phys 1990;68:1825–30.
[13] Swanepoel R. J Phys E 1983;16:1214–22.
[14] Márquez E, Nagels P, González-Leal JM, Bernal-Oliva AM, Sleeckx E, Callaerts R. Vacuum 1999;52(1–2):55–60.
[15] Tigau N, Ciupina V, Prodan G. J Cryst Growth 2005;277(Issues 1–4):529–35.
[16] Ray S, Banerjee R, Basu N, Batabyal AK, Barua AK. J Appl Phys 1983;54:3497.
[17] Burstein E. Phys Rev C 1954;93:632.
[18] Weihtens CHL, Van Loon PAC. Thin Solid Films 1991;196:1.